

## Video Article

# The Diffusion of Passive Tracers in Laminar Shear Flow

Manuchehr Aminian<sup>1,2</sup>, Francesca Bernardi<sup>1</sup>, Roberto Camassa<sup>1</sup>, Daniel M. Harris<sup>1,3</sup>, Richard M. McLaughlin<sup>1</sup><sup>1</sup>Department of Mathematics, University of North Carolina at Chapel Hill<sup>2</sup>Department of Mathematics, Colorado State University<sup>3</sup>School of Engineering, Brown UniversityCorrespondence to: Roberto Camassa at [camassa@amath.unc.edu](mailto:camassa@amath.unc.edu), Daniel M. Harris at [daniel\\_harris3@brown.edu](mailto:daniel_harris3@brown.edu), Richard M. McLaughlin at [rmm@email.unc.edu](mailto:rmm@email.unc.edu)URL: <https://www.jove.com/video/57205>DOI: [doi:10.3791/57205](https://doi.org/10.3791/57205)

Keywords: Engineering, Issue 135, Passive tracer advection, microfluidics, diffusion, symmetry breaking, skewness, Monte Carlo, experimental fluid dynamics

Date Published: 5/1/2018

Citation: Aminian, M., Bernardi, F., Camassa, R., Harris, D.M., McLaughlin, R.M. The Diffusion of Passive Tracers in Laminar Shear Flow. *J. Vis. Exp.* (135), e57205, doi:10.3791/57205 (2018).

## Abstract

A simple method to experimentally observe and measure the dispersion of a passive tracer in a laminar fluid flow is described. The method consists of first injecting fluorescent dye directly into a pipe filled with distilled water and allowing it to diffuse across the cross-section of the pipe to obtain a uniformly distributed initial condition. Following this period, the laminar flow is activated with a programmable syringe pump to observe the competition of advection and diffusion of the tracer through the pipe. Asymmetries in the tracer distribution are studied and correlations between the pipe cross-section and the shape of the distribution is shown: thin channels (aspect ratio  $\ll 1$ ) produce tracers arriving with sharp fronts and tapering tails (front-loaded distributions), while thick channels (aspect ratio  $\sim 1$ ) present the opposite behavior (back-loaded distributions). The experimental procedure is applied to capillary tubes of various geometries and is particularly relevant to microfluidic applications by dynamical similarity.

## Video Link

The video component of this article can be found at <https://www.jove.com/video/57205/>

## Introduction

In recent years, substantial efforts have been focused on developing microfluidic and lab-on-chip devices that can reduce the costs and increase the productivity of chemical preparation and diagnostics for a range of applications. One of the main features of microfluidic devices is the pressure-driven transport of fluids and dissolved solutes through microchannels. In this context, it has become increasingly important to better understand the controlled delivery of solutes at the microscale. In particular, applications such as chromatographic separation<sup>1,2</sup> and microfluidic flow injection analysis<sup>3,4</sup> require improved control and understanding of solute delivery. Researchers in microfluidics have studied and documented the influence of the channel's cross-sectional shape on solute spreading<sup>5,6,7,8</sup>, and the role of the channel's aspect ratio<sup>9,10</sup>.

Analytical and numerical studies of solute spreading along channels have recently lead to the identification of a correlation between the pipe cross-sectional geometry and the shape of the distribution<sup>9,10</sup>. At early timescales, the distribution strongly depends on the geometry: rectangular pipes break symmetry almost immediately, while elliptical pipes retain their initial symmetry much longer<sup>9</sup>. On the other hand, progressing into longer timescales the asymmetries in the solute distribution no longer differentiate ellipses from rectangles, and are set solely by the cross-sectional aspect ratio  $\lambda$  (ratio of the short to long side). Considering "pipes" of elliptical cross-sections and "ducts" of rectangular cross-sections, predictions from numerical simulations and asymptotic analysis were benchmarked with laboratory experiments. Thin channels (aspect ratio  $\ll 1$ ) produce solutes arriving with sharp fronts and tapering tails, while thick channels (aspect ratio  $\sim 1$ ) present the opposite behavior<sup>10</sup>. This robust effect is relatively insensitive to the initial conditions and can be used to help select the solute distribution profile required for any application.

The behavior outlined above of sorting thin versus thick domains happens before the classical "Taylor dispersion" regime is reached. Taylor dispersion refers to the enhanced spreading of passive solutes in laminar flow (stable at low Reynolds number,  $Re$ ) with a boosted effective diffusivity, inversely proportional to the solute's molecular diffusivity  $\kappa$ <sup>11</sup>. This enhancement is observed only after long, diffusive timescales, when the solute has diffused across the channel. Such diffusive timescale is defined in terms of the characteristic length scale  $a$  of the geometry, as  $t_d = a^2/\kappa$ . The Péclet number is a nondimensional parameter which measures the relative importance of fluid advection to diffusion effects. We define this parameter in terms of the shortest length scale as  $Pe = Ua/\kappa$ , where  $U$  is the characteristic flow speed. (The Reynolds number can be defined in terms of the Péclet number as  $Re = Pe \kappa/\nu$ , where  $\nu$  is the kinematic viscosity of the fluid.) Typical Péclet number values for microfluidic applications<sup>12</sup> vary between 10 and  $10^5$ , with molecular diffusivities ranging from  $10^{-7}$  to  $10^{-5}$  cm<sup>2</sup>/s. Hence, given the flow speeds and length scales of interest, it is critical to understand the behavior of solutes for intermediate-to-long timescales (relative to the diffusive timescale), well past the initial observations of geometry-driven behavior and into the cross-section-driven regimes universal for a large class of geometries.

Given the interest in microfluidic applications, the choice of a large scale experimental setup may at first seem unnatural. The experiments reported herein are at the millimeter scale, not at the microscale as in true microfluidic devices. However, the same physical behaviors characterize both systems and a quantitative study of the relevant phenomena can still be achieved by properly scaling the governing equations, just as scale models of aircraft are assessed in wind tunnels during the design phase. In particular, matching relevant nondimensional parameters (such as the Péclet number for our experiment) ensures the adaptability of the experimental model. Working at such larger scales, while maintaining a laminar pressure-driven flow, offers several advantages over a traditional microscale setup. In particular, the equipment required to manufacture, perform, and visualize the present experiments is easier to operate and less costly. Furthermore, other common challenges of working with microchannels, such as frequent clogging and the enhanced influence of manufacturing tolerances, are mitigated with the larger setup. Another possible use for this experimental setup is for studies of residence time distribution (RTD) in laminar flows<sup>13</sup>.

The asymmetries arising in the solute distribution downstream can be analyzed via its statistical moments; in particular, the skewness, which is defined as the centered, normalized third moment, is the lowest order integral statistic measuring the asymmetry of a distribution. The sign of the skewness typically indicates the shape of the distribution, *i.e.* if it is front-loaded (negative skewness) or back-loaded (positive skewness). Focusing on the aspect-ratios of the channels, there exists a clear correlation of thin geometries with front-loaded distributions, and thick geometries with back-loaded distributions<sup>10</sup>. Additionally, a critical aspect ratio separating these two opposite behaviors can be calculated for both elliptical pipes and rectangular ducts. Such crossover aspect ratios are remarkably similar for standard geometries, in particular,  $\lambda^* = 0.49031$  for pipes, and  $\lambda^* = 0.49038$  for ducts, suggestive of the universality of the theory<sup>10</sup>.

The experimental setup and method described in this paper are used to study the spreading of a pressure-driven passive solute in laminar fluid flows throughout glass capillaries of various cross-sections. The simplicity and reproducibility of the experiment defines a robust method of analysis for understanding the connection between a pipe's geometrical cross-section and the resulting shape of the injected solute distribution as it is transported downstream. The method discussed in this work has been developed to readily benchmark mathematical and numerical results in a physical laboratory setting.

A simple experimental procedure is described which highlights the definitive role played by a fluidic channel's cross-sectional aspect-ratio in setting the shape of a solute distribution downstream. The experimental setup requires a programmable syringe pump to produce a laminar steady flow, smooth glass pipes of various cross-sections, a second syringe pump to inject the diffusing solute (*e.g.* fluorescein dye) into the surrounding laminar flow, and UV-A lights and a camera to record the solute evolution. CAD files are provided for all the custom parts of the setup and such files can be used to 3D-print the experimental parts prior to assembly.

## Protocol

### 1 . Prepare the parts to build the experimental setup

- Utilize the 3D CAD drawings attached (.stl format) to 3D-print an injector post, a reservoir, a hexagonal connector, and two plates to be used as mounts for the pipes (two for each geometry).  
NOTE: Alternatively, certain parts of the setup can be laser-cut. In this report, the square thick pipe has been mounted with laser-cut plates, while the rectangular thin pipe has been mounted with 3D-printed plates.
- Obtain smooth glass capillary pipes of the desired geometry.  
NOTE: In this report, two pipe geometries are used: 30 cm-long pipe of square cross-section - internal cross-section 1 mm x 1 mm and wall thickness 0.2 mm; 30 cm-long pipe of rectangular cross-section - internal cross-section 1 mm x 10 mm and wall thickness 0.7 mm. The square pipe is henceforth referred to as the thick pipe, whereas the rectangular pipe is referred to as the thin pipe.

### 2 . Assembly of the experimental setup

- Tapping of the 3D-Printed parts
  - Tap the injector post on both sides with a 1/8" (0.32 cm) NPT tap where the injection needle and dye input will be installed. Tap the reservoir in the back with a 10-32 tap where the draining tube will be installed.
  - Tap the four screw holes with a 6-32 tap on the front of the reservoir. Tap the hexagonal connector piece on the top and bottom with a 6-32 tap.
- Prepare the tapped 3D-printed parts
  - Injector post
    - Cover the threads of a barbed hose fitting with PTFE sealing tape. Screw the prepared fitting onto the back hole of the injector post. Cut a 30 cm-long piece of plastic tubing (inner diameter 3.30 mm). Insert the tube on the hose adaptor.
    - Cover the threads of the stainless-steel dispensing needle (outer diameter 0.71 mm) with PTFE sealing tape. Screw the stainless-steel dispensing needle on the front (large) hole onto the injector post.
  - Reservoir
    - Cover the threads of a small barbed hose fitting with PTFE sealing tape. Screw the prepared fitting onto the back hole of the reservoir (smaller hole).
    - Cut a 30 cm-long piece of plastic tubing (inner diameter 3.30 mm). Insert the tube onto the hose adaptor. Close the other end of the tube with a small cap.  
NOTE: This will be the draining system for the reservoir.
    - Place a rubber O-Ring (Oil-Resistant Buna-N O-Ring, 1/16" (0.16 cm) Fractional Width, Dash Number 016) in the circular recession on the pipe side of the reservoir.
- Hexagonal connector

1. Cover the threads of a small barbed hose fitting with PTFE sealing tape. Screw the prepared fitting onto the bottom hole of the hexagonal connector.
  2. Cut a 30 cm-long piece of plastic tubing (inner diameter 3.30 mm). Insert the tube on the hose adaptor.
  3. Cover a hose adaptor with PTFE sealing tape. Make sure to cover the hose adaptor going against the threads.
  4. Cut a 4 cm-long piece of plastic tubing (inner diameter 3.30 mm). Insert the tube on the hose adaptor.
3. Prepare the pipe
1. Distribute a thin layer of RTV rubber sealant 2 mm away from each end of the pipe. Spread the sealant evenly around the outside of the pipe and make sure not to obstruct the pipe access with the sealant.
  2. Mount the pipe onto the 3D-printed plates by inserting it carefully into the pre-cut holes on the 3D-printed pipe adapters. Make sure to push the pipe in at least 2 mm so that the sealant along each side contacts with the plates.
  3. Carefully spread the sealant onto the edge of the plate so that the pipe gets sealed into the cutout. Wait at least 12 h for the sealant to fully vulcanize thus sealing the pipe onto the plates.
4. Measure 0.40 g of fluorescein powder to prepare the dye solution. Dilute powder into 0.50 L of distilled water to obtain the desired dye concentration (0.80 g/L concentration).  
NOTE: The diffusivity of fluorescein in water is estimated by performing a least-squares fit of the analytical expression for the second moment of the cross-sectionally averaged tracer distribution in the circular pipe geometry<sup>14</sup> to the experimental measurement of the same quantity. The molecular diffusion coefficient is estimated to be  $\kappa = 5.7 \times 10^{-6} \text{ cm}^2/\text{s}$ , consistent with previously published values of diffusivity of fluorescein in pure water.
5. Assembly
1. Syringe pump A setup
    1. Fill a 12 mL plastic syringe with a rubber plunger with distilled water. Insert a plastic dispensing tip onto the syringe. Mount the syringe onto syringe pump A. Connect the syringe to the 30 cm-long tube inserted at the bottom of the hexagonal connector.
    2. Fill a 1 mL plastic syringe with a rubber plunger with distilled water. Mount the syringe onto syringe pump A. Cut a 30 cm-long piece of plastic tubing (inner diameter 3.30 mm). Attach it to the 1 mL plastic syringe.  
NOTE: Both syringes filled with distilled water are mounted on syringe pump A. As the pump is activated, water will be ejected from both syringes. The first one to be used is the 12 mL syringe, so the 1 mL syringe needs to be connected to a draining tube to avoid water spills. This step is not necessary for the thin rectangular pipe.
  2. Injector Setup
    1. Fill a 3 mL plastic syringe with a rubber plunger with the fluorescein solution. Insert a plastic dispensing tip onto the syringe.
    2. Attach the tube connected to the back of the injector to the dye syringe.
    3. Fill the injector post with the dye solution by manually injecting dye through the syringe while holding the injector post horizontally (*i.e.* with the needle oriented upwards and above the syringe). Keep pushing on the syringe until the injector is completely full of dye and no air is trapped inside.
    4. Mount the syringe onto syringe pump B. Clamp the injector post to the edge of the lab bench in a way that it is reachable by the tube connected to the syringe pump.
    5. Insert small washers on four long screws (Stainless Pan Head Phillips Machine Screws 6-32 Thread, 2-1/4" (5.76 cm) length). Insert the four screws in the four holes surrounding the needle.  
NOTE: Make sure the head of the screw is on the back of the injector post (on the same side as the tube connected to the dye syringe).
  3. Hexagonal connector
    1. Place two O-Rings (Oil-Resistant Buna-N O-Ring, 1/16" (0.16 cm) Fractional Width, Dash Number 016) in the circular cutouts on each side of the hexagonal connector.
    2. Attach the hexagonal connector to the injector post by aligning its holes to the four screws and inserting it on them. Make sure to have the side with the larger hole facing the injector post. Check and ensure that the O-Ring does not move out of place when clamped between the two parts.
  4. Pipe
    1. Attach one of the end-plates connected to the pipe to the hexagonal connector by aligning its holes to the four screws and inserting it onto them. Pay close attention to the needle which needs to enter the pipe as it is being mounted.
    2. Secure the four long screws to compress together the injector, the hexagonal connector, and the pipe-adaptor plate by attaching four 6-32 stainless steel nuts to the end of the long bolts. Ensure that the O-Rings do not move out of place when clamped between the parts.
    3. Attach the opposite end of the pipe to the reservoir by using four short screws and washers (Stainless Pan Head Phillips Machine Screws 6-32 Thread, 1/2" (1.27 cm) length). Check that the O-Ring does not move out of place when compressed between the two parts.
  5. Clamp the reservoir to the table. Make sure the reservoir is aligned with the injector post to not bend the pipe.
  6. Air extraction system: Insert a plastic dispensing tip into the tube connected to the top of the hexagonal connector. Attach a 3 mL syringe to the plastic tip.  
NOTE: This syringe will be used to extract any air bubbles trapped in the system.
  7. Lights and Camera
    1. Place two 61 cm-long UV-A tube lights on each side of the experimental setup.  
NOTE: There is a specifically designed track on each side of both the injector and reservoir. The experiment should be run in the dark with the UV-A tube lights turned on.
    2. Place a camera with memory card above the experimental setup facing down.

NOTE: The camera should be positioned at least 1 m above the pipe. In this way, the frame will include the entire pipe length. A DSLR camera was used with a lens of adjustable focal length, 24 - 120 mm.

3. Program the camera using a remote trigger to take pictures every 1 s with aperture 5.6f, shutter speed 5, and ISO 200.

### 3. Experimental run

#### 1. Setup

1. Fill the reservoir with distilled water to a level slightly above the pipe. Fill pipe with distilled water by pushing on the syringe pump. Turn on the UV-A tube lights and pull the blackout curtains.
2. Run the programmable syringe pump A to flush the pipe of any residual dye.
3. Take a single reference image of the pipe filled with pure distilled water.  
NOTE: This is the reference shot that will be used in the data processing steps later. This picture needs to be taken in the dark in conditions as similar as possible to the experimental run.
4. Switch the tube connecting to the injector post to the 1 mL syringe mounted on syringe pump A. Connect the 12 mL syringe to the draining tube (previously connected to the 1 mL syringe).  
NOTE: This step is not necessary for the thin rectangular pipe.

#### 2. Initial Condition

1. Inject a 1 mm-thick dollop of dye (3 mm-thick for the thin rectangular tube) in the pipe by running the analog syringe pump B.  
NOTE: This step creates the dye initial condition. The amount of dye injected depends on the geometry of the pipe used. The thin tube requires a larger amount of dye because its cross-sectional area is larger. Before the experimental run, the dye will have to diffuse across the cross-section and injecting a larger amount of dye ensures that it will be bright enough to be captured in photographs even after it has diffused.
2. Program syringe pump A to inject distilled water at the very slow flow rate of 0.193 mL/h for the thick square pipe (the flow rate is 1.93 mL/h for the thin rectangular pipe). Run the syringe pump for 5 min to allow the bolus of dye to be transported down the pipe away from the needle.  
NOTE: After 5 min, the dye should be approximately 1 cm away from the needle. The increase in the flow rate by one order of magnitude for the thin pipe is because the volume of the thin pipe is 10 times that of the thick pipe.
3. Pull the dye syringe backwards manually, making sure the dye does not reach the needle.  
NOTE: This will ensure that there is distilled water at the end of the needle so that no more dye will be dispersed into the pipe during the experimental run.
4. Wait for a time  $t_w > t_d^*$  for the dye bolus to diffuse across the cross-section of the pipe.  
NOTE: The diffusive time  $t_d^* = b^2/k$  considers the characteristic length  $b$  to be half the long cross-sectional side. This way of computing the wait time is generalizable to any cross-section with an appropriate choice of  $b$ . For our representative results, the wait time was 15 min for the thick square pipe and 15 h for the thin rectangular pipe.

#### 3. Flow

1. Program syringe pump A to the desired flow rate of 1.93 mL/h for the thick square pipe and 19.3 mL/h for the thin rectangular pipe.
2. Start the syringe pump and the remote trigger on the camera at the same time. Run the experiment for 5 min, with an interval between pictures of 1 s.
3. Turn the room lights on and take an image of a ruler placed at the same height as the pipe and parallel to it.  
NOTE: This will help determine the length scale (pixels/mm) used in data processing.

### 4. Data Processing

1. Extract the memory card from the camera and download the data to a computer where image processing software will be used to analyze it.
2. MATLAB analysis
  1. First subtract the reference image shot (snapped in step 3.1.3) from the first experimental image.
  2. Crop the image along the upper and lower edges of the pipe. Make sure to rotate the image if the pipe is not aligned with the frame.
  3. Sum the intensity reading of the green channel vertically in the resulting image.  
NOTE: This is proportional to the total cross-sectional dye intensity as a function of the length along the pipe.
  4. Convert the units of length from pixels to mm by using the physical length scale from the calibration image (see step 3.3.3).
  5. Repeat for all remaining images. This results in a time sequence of the curves measuring the total dye concentration along the length of the pipe.

### Representative Results

The experimental setup after assembly is shown in **Figure 1**. Images produced in MATLAB show the experimental data above the processed evolution of the concentration curve (**Figure 2**) for three non-dimensional times. We have verified that there is a linear relation between the tracer's intensity and concentration. The shape of the distribution changes as time passes and the dye bolus moves downstream. **Figure 2** shows such evolution in the case of the thin rectangular duct geometry. The initial dye distribution is narrow and symmetric (Gaussian-like with respect to the longitudinal direction and nearly uniform in the cross-section, **Figure 2** left), but the symmetry is broken almost immediately as the background flow starts. The distribution breaks symmetry by presenting a sharp front and long tapering tails (**Figure 2**, middle and right).

The experimental results are confirmed by Monte Carlo simulations performed matching the initial distribution and flow rate (**Figure 3**). The fitted value for the dye diffusivity  $\kappa$  was determined in an independent experiment (step 2.4 in protocol) and used in this comparison. Monte Carlo methods are often used to simulate the evolution of advection-diffusion problems involving complex geometries as the boundary conditions (homogeneous Neumann in this case) can be simply input as billiard like reflection rules. The approach is to sample realizations of the equivalent stochastic differential equation underlying the advection-diffusion equation in nondimensional form:

$$\frac{\partial T}{\partial \tau} + Pe u(y, z) \frac{\partial T}{\partial x} = \Delta T$$

where  $T(x, y, z, t)$  is the tracer distribution,  $\tau$  is the nondimensional time normalized by  $t_d$ ,  $x$  is the longitudinal spatial coordinate,  $y$  is the short transverse coordinate, and  $z$  is the long transverse coordinate, all normalized by the short side  $a$ . The fluid flow  $u(y, z)$  is the laminar steady-state solution to the Navier-Stokes equations with no-slip boundary conditions (no flow at the wall), driven by a negative pressure gradient. A Gaussian initial data in the pipe longitudinal direction with a desired variance can be obtained by considering only diffusion ( $Pe = 0$ ) and evolving the particles for the desired time to match the width of the experimental initial data<sup>9,10</sup>. These representative results were obtained using the flow rate values specified in the protocol, however we expect the loading phenomena observed to hold in general for the laminar regime<sup>10</sup> (**Figure 3**).

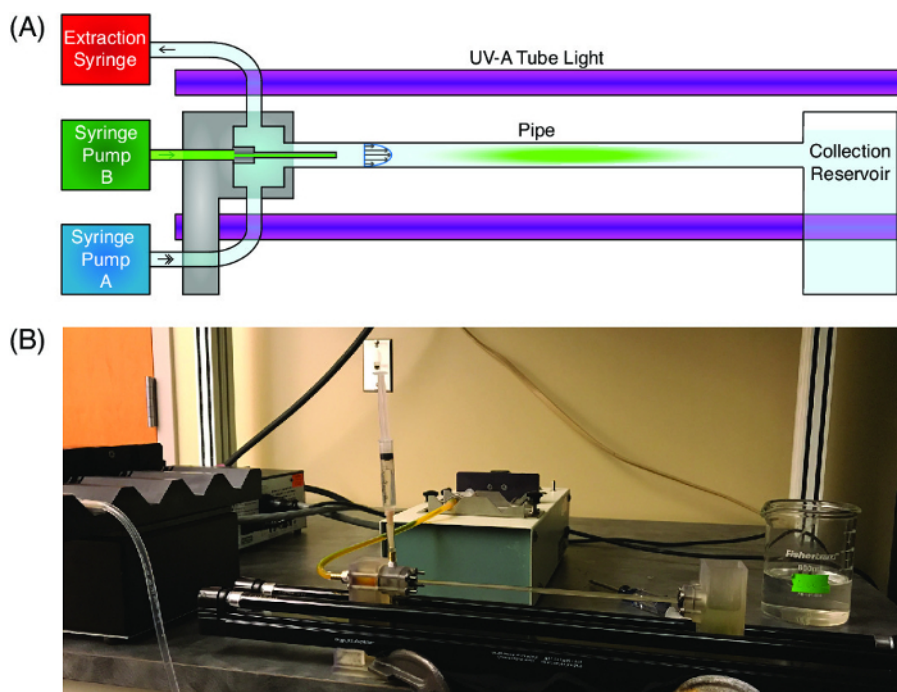


**Figure 1: Experimental setup.** (A) Diagram of the experimental setup. This figure has been modified from Aminian *et al.*<sup>10</sup>. (B) Presentation of the actual setup. [Please click here to view a larger version of this figure.](#)

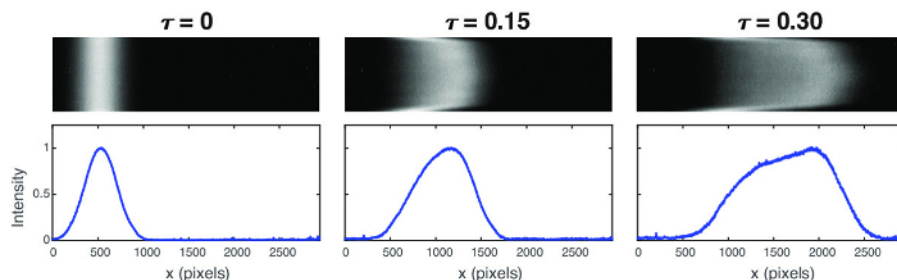


**Figure 2: Snapshots of processed data at various times.** Top row: photo of the dye concentration diffused along the cross-section of the tube observed normally to the long cross-sectional direction at increasing non-dimensional times. The vertical axis has been scaled 5 times for the sake of clarity. Bottom: intensity of the dye concentration computed summing along the long cross-sectional direction. The peak value is normalized. [Please click here to view a larger version of this figure.](#)

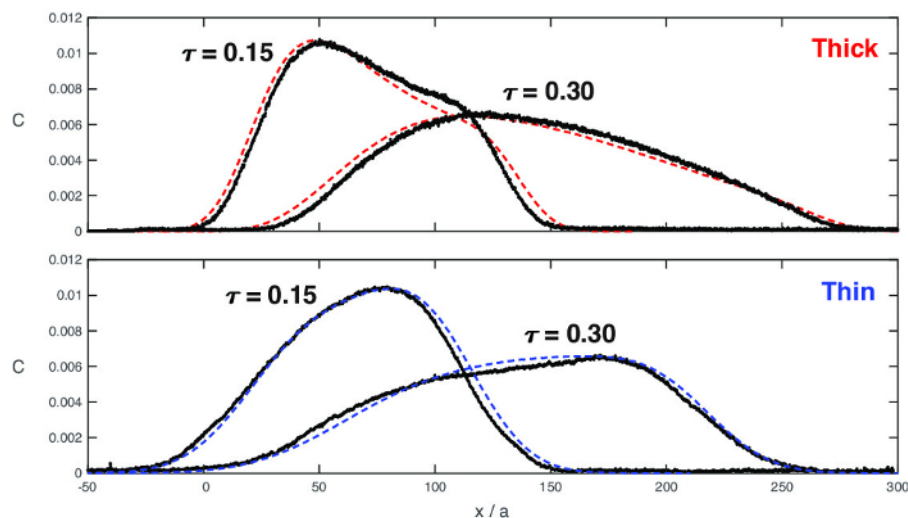


**Figure 3: Comparison of the concentration distribution between Monte Carlo simulations and experiments.** The evolution of the cross-sectionally averaged dye concentration along the longitudinal length of the pipe is shown at two instants in time:  $\tau = 0.15$  and  $\tau = 0.30$ . The dashed lines are the simulation results, while the solid lines represent the experimental data. Top: comparison in the thick (square) channel; bottom: comparison in the thin (rectangular) channel. The area under each curve is normalized to be one and  $x = 0$  corresponds to the center of the initial plug of dye. This figure has been modified from Aminianet *et al.*<sup>10</sup>. [Please click here to view a larger version of this figure.](#)

**Supplementary File 1.** Included CAD drawings of 3D Hexagonal Connector ([hex\\_connector\\_3D.STL](#))

**Supplementary File 2.** Included CAD drawings of 3D Injector Post ([injector\\_post\\_3D.STL](#))

**Supplementary File 3.** Included CAD drawings of 3D Reservoir ([reservoir\\_3D.STL](#))

**Supplementary File 4.** Included CAD drawings of 3D Thick Pipe Plates ([plate\\_thick\\_3D.STL](#))

**Supplementary File 5.** Included CAD drawings of 3D Thin Pipe Plates ([plate\\_thin\\_3D.STL](#))

## Discussion

After injecting dye into the pipe, the bolus is transported away from the injection needle using a steady flow. Then, it is necessary to wait long enough for the dye to diffuse across the cross-section of the channel. In this way, a uniform Gaussian-like distribution is obtained and will serve as the initial condition for the experiment. Hence, a laminar background flow is created with the programmable syringe pump. The experimental run lasts for 5 min with photos taken every second.

The most common issues in the setup come from the connection of the parts and the pipes. The various 3D-printed parts need to be sealed properly when connected to avoid leaking. The glass pipes are very delicate and must be handled and installed with care.

An issue we encountered when transitioning from the thin rectangular pipe to the thick square pipe was related to the fact that the pipe volume was reduced by a factor of 10. To maintain the same cross-sectional average flow speed with the mounted 12 mL syringe, the plunger speed in syringe pump A would have needed to be extremely low. At this programmed speed, the plunger velocity was not uniform anymore and a steady flow cannot be guaranteed throughout the experimental run. Therefore, we switched to a much smaller 1 mL syringe when working with the thick square pipe in step 2.5.1.

Also, one should verify that the average intensity along the vertical dimension of the pipe in the initial condition is approximately uniform. If not, a filtering mask needs to be applied across all frames to account for this discrepancy.

The least repeatable part of the experiment is the dye injection (and consequently the width of the initial distribution). As illustrated earlier, it is not a concern for matching with the Monte Carlo simulations, as the experimental initial condition can be recreated using the analysis of the initial photograph. The dye injection and consequent manual withdrawing may not always produce dye plugs of precisely the same width. Particular care needs to be applied when setting up the initial dye bolus. The experiment becomes more repeatable as researchers gain experience in this part of the protocol, but future improvements could certainly be made.

When comparing the setup with microfluidic devices, the only parameter that appear in the governing equation when appropriately nondimensionalized is the Péclet number  $Pe$  if the tracer is passive, *i.e.* the tracer evolution is uncoupled from the flow. Dynamic similarity is implicit in the assumption of low Reynolds ( $Re \ll 1$ ) which ensures stable laminar flows  $u(y,z)$ . These two parameters are setting the full similarity between microfluidic setups and the scales of our experiment. In practice, the physical length of the pipe only restricts the nondimensional times we can safely reach with our setup. For very late non-dimensional times, the necessary length of the pipe could become prohibitively long for a fixed Péclet number in this large-scale setup.

An obvious limitation of this experimental protocol is that the data collected is a projected 2D representation of 3D geometry as the pictures are taken top-down on the pipe. The current process only allows to obtain the evolution of the cross-sectionally averaged dye distribution. Obtaining

a distribution defined at each location in the tube rather than on its cross-sectional average and comparison with theoretical and numerical predictions are the subject of ongoing research.

All the experimental setup parts have technical drawings available for download which makes the setup easily accessible and customizable by any interested researcher. Building on the current results, the same setup will be used to study more complex and unexplored pipe geometries as well as different flow regimes.

## Disclosures

The authors have nothing to disclose.

## Acknowledgements

We acknowledge funding from the Office of Naval Research (grant DURIP N00014-12-1-0749) and the National Science Foundation (grants RTG DMS-0943851, CMG ARC-1025523, DMS-1009750, and DMS-1517879). Additionally, we acknowledge the work of Sarah C. Burnett who helped develop an early version of the experimental setup and protocol.

## References

1. Dutta, D., Leighton Jr., D. T. Dispersion in Large Aspect Ratio Microchannels for Open-Channel Liquid Chromatography. *Anal. Chem.* **75**(1), 57-70 (2003).
2. Blom, M. T., Chmela, E., Oosterbroek, R. E., Tijssen, R., van den Berg, A. On-Chip Hydrodynamic Chromatography Separation and Detection on Nanoparticles and Biomolecules. *Anal. Chem.* **75**(24), 6761-6768 (2003).
3. Betteridge, D., Fields, B. Construction of pH Gradients in Flow-Injection Analysis and Their Potential Use for Multielement Analysis in a Single Sample Bolus. *Anal. Chem.* **50**(4), 654-656 (1978).
4. Trojanowicz, M., Kołacińska, K. Recent advances in flow injection analysis. *Analyst.* **141**, 2085-2139 (2016).
5. Ajdari, A., Bontoux, N., Stone, H. A. Hydrodynamic Dispersion in Shallow Microchannels: The Effect of Cross-Sectional Shape. *Anal. Chem.* **78**(2), 387-392 (2006).
6. Dutta, D., Ramachandran, A., Leighton Jr., D. T. Effect of channel geometry on solute dispersion in pressure-driven microfluidic systems. *Microfluid Nanofluid.* **2**(4), 275-290 (2006).
7. Bontoux, N., Pépin, A., Chen, Y., Ajdari, A., Stone, H.A. Experimental characterization of hydrodynamic dispersion in shallow microchannels. *Lab Chip.* **6**, 930-935 (2006).
8. Vedel, S., Bruus, H. Transient Taylor-Aris dispersion for time-dependent flows in straight channels. *J. Fluid Mech.* **691**, 95-122 (2012).
9. Aminian, M., Bernardi, F., Camassa, R., McLaughlin, R.M. Squaring the Circle: Geometric Skewness and Symmetry Breaking for Passive Scalar Transport in Ducts and Pipes. *Phys. Rev. Lett.* **115**, 154503 (2015).
10. Aminian, M., Bernardi, F., Camassa, R., Harris, D.M., McLaughlin, R.M. How boundaries shape chemical delivery in microfluidics. *Science.* **354**(6317), 1252-1256 (2016).
11. Taylor, G.I. Dispersion of soluble matter in solvent flowing slowly through a tube. *P Roy Soc Lond A Mat.* **219**(1137), 186-203 (1953).
12. Stone, H.A., Stroock, A.D., Ajdari, A. Engineering Flows in Small Devices: Microfluidics Toward a Lab-on-a-Chip. *Annu. Rev. Fluid Mech.* **36**, 381-411 (2004).
13. Davis, M.E., Davis, R.J. *Fundamentals of chemical reaction engineering*. McGraw-Hill Higher Education. New York, NY (2003).
14. Barton, N. On the method of moments for solute dispersion. *J. Fluid Mech.* **126**, 205 (1983).